CHEMMEDCHEM

ChemPubSoc Europe

DOI: 10.1002/cmdc.201200348

Aromatic Core Extension in the Series of N-Cyclic Bay-Substituted Perylene G-Quadruplex Ligands: Increased Telomere Damage, Antitumor Activity, and Strong Selectivity for Neoplastic over Healthy Cells

Marco Franceschin,[a] Angela Rizzo,[b] Valentina Casagrande,[a] Erica Salvati,[b] Antonello Alvino,[a] Alessandro Altieri,[a] Alina Ciammaichella,[a] Sara Iachettini,[b] Carlo Leonetti,[b] Giancarlo Ortaggi,[a] Manuela Porru,[b] Armandodoriano Bianco,*[a] and Annamaria Biroccio*[b]

Based on previous work on both perylene and coronene derivatives as G-quadruplex binders, a novel chimeric compound was designed: *N*,*N*′-bis[2-(1-piperidino)-ethyl]-1-(1-piperidinyl)-6-[2-(1-piperidino)-ethyl]-benzo[ghi]perylene-3,4:9,10-tetracarboxylic diimide (EMICORON), having one piperidinyl group bound to the perylene bay area (positions 1, 12 and 6, 7 of the aromatic core), sufficient to guarantee good selectivity, and an extended aromatic core able to increase the stacking interactions with the terminal tetrad of the G-quadruplex. The obtained "chimera" molecule, EMICORON, rapidly triggers extensive DNA damage of telomeres, associated with the delocalization of telomeric protein protection of telomeres 1 (POT1), and efficiently limits the growth of both telomerase-positive and -negative tumor cells. Notably, the biological effects of EMICORON are more potent than those of the previously described perylene derivative (PPL3C), and more interestingly, EMICORON appears to be detrimental to transformed and tumor cells, while normal fibroblasts expressing telomerase remain unaffected. These results identify a new promising G-quadruplex ligand, structurally and biologically similar on one side to coronene and on the other side to a bay-monosubstituted perylene, that warrants further studies.

Introduction

G-quadruplexes (G4) are non-canonical secondary structures formed in DNA sequences containing consecutive runs of guanines that are thought to play a role in key biological processes including telomere maintenance.[1] These findings have prompted a search for small organic molecules as specific ligands for these structures, for their development as potential anticancer agents.[2] The number of known G4 ligands has grown rapidly over the past few years.[3] Features shared by many of these ligands include an aromatic core that favors stacking interactions with the G-tetrads, and, in most cases, basic side chains that interact with the quadruplex grooves.[4] Despite the promising results obtained in preclinical models, only two drugs that target either a G4 (Quarfloxin) or fold into a G4 structure (AS1411) are presently in phase II clinical trials.[5]

G4 ligands were initially designed to counteract telomerase action at telomeres. Surprisingly, their antiproliferative effects can occur in telomerase-negative cells and follow kinetics, which cannot be merely explained by telomere shortening, suggesting that these compounds affect other pathways that are not necessarily related to telomere biology. Results from different research groups,[6] including ours,[7] clearly demonstrated that, in addition to their telomerase inhibitory properties, these drugs can exert an anticancer effect by telomeric chromatin alteration, leading to the activation of damage foci (i.e., γH2AX, p53 binding protein 1 (53BP1)) that co-localize with the telomeric repeats. It emerged that G4-interacting agents are more than simple telomerase inhibitors and that their direct target is telomere instead of telomerase.

Our group recently reported an N-cyclic bay-monosubstituted perylene diimide **1** (PPL3C, Figure 1) as a selective G4 ligand able to induce a specific telomere damage and antiproliferative activity on both transformed and tumor cells.[8] In particular, we pointed out that the presence of bulky groups on the perylene bay area (positions 1, 12 and 6, 7) gives a good selectivity with respect to duplex DNA, which was missing in previously reported unsubstituted perylene diimides. Furthermore, we found that only one piperidinyl group is necessary to give such selectivity, whereas the second piperidinyl group

[a] *Dr. M. Franceschin,[+] Dr. V. Casagrande, Dr. A. Alvino, Dr. A. Altieri, Dr. A. Ciammaichella, Prof. G. Ortaggi, Prof. A. Bianco*
Dipartimento di Chimica
Sapienza Università di Roma
P.le A. Moro 5, 00185 Roma (Italy)
E-mail: Armandodoriano.Bianco@uniroma1.it

[b] *Dr. A. Rizzo,[+] Dr. E. Salvati, Dr. S. Iachettini, Dr. C. Leonetti, Dr. M. Porru, Dr. A. Biroccio*
Experimental Chemotherapy Laboratory
Regina Elena National Cancer Institute
Via delle Messi d'Oro 156, 00158 Rome (Italy)
E-mail: biroccio@ifo.it

[+] *These authors contributed equally to the paper.*

Supporting information for this article is available on the WWW under http://dx.doi.org/10.1002/cmdc.201200348.

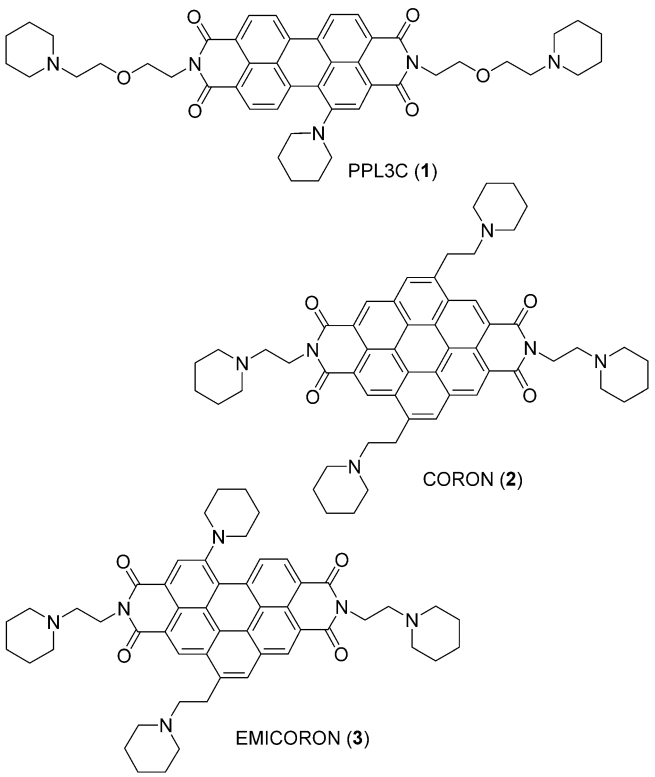

Figure 1. Chemical structures of N-cyclic bay-substituted perylene and coronene derivatives. "Chimera" molecule **3** has one half similar to coronene and the other half similar to bay-monosubstituted perylene.

hinders the interaction with the terminal quadruplex G-tetrad.[8] For these reasons, a bay-monosubstituted perylene diimide such as **1** is characterized by decreased steric hindrance, which (compared with other derivatives with two bulky substituents on the bay area) enables improved overlap on the terminal G-tetrad to occur. From a structural point of view, we noticed that the second bay area of monosubstituted perylene diimides was free to be derivatized. Therefore, it may be interesting to enlarge the planar aromatic area on this side of the molecule, to improve interaction with the terminal G-tetrad, provided that the selectivity with respect to duplex DNA should be granted by the presence of the piperidinyl group on the other side.

In fact, we previously reported a series of hydrosoluble coronene derivatives, which are characterized by a large hydrophobic aromatic core, as G4 ligands and telomerase inhibitors.[9] By using ESI-MS, we showed that coronene derivatives have a much higher capability of binding to G4 DNA than two side-chain perylene derivatives,[10] in agreement with the idea that a larger aromatic core should give better interaction with the G-tetrads.[4] Specific biological and molecular assays have been performed on the reference compound of this series 2 (CORON (**2**), Figure 1); we found that this G4 ligand is highly active, in terms of inhibition of cell proliferation on both transformed- and tumor cells, but this effect also occurs in normal telomerized fibroblasts (see Table S1 and Figure S1 A and B in the Supporting Information). In agreement with these results, compound **2** induces DNA damage, both in normal and transformed cells, even if, consistently with the previously reported high capability of **2** to bind G4 versus duplex DNA,[10d] DNA damage is also localized at the telomeric regions (see Figure S1 C and D in the Supporting Information). These results suggest that **2** can also interact with additional targets outside the telomere and indicates that it can have off-target effects.

Following these considerations, we designed a "chimera" molecule, in which one half is similar to coronene and for the other half to a bay-monosubstituted perylene (EMICORON (**3**), Figure 1).

Results

Synthesis

Starting compound **4** (PIPER-Br) was prepared as previously described.[11] A small amount (no more than 10% at this stage) of the 1,6-isomer was always present, which was determined by analyzing the ^{1}H NMR spectra, as discussed in the cited literature. In Scheme 1, only the isomer **4** and the relative subsequent products are shown. The first step was the selective substitution of only one bromine atom with piperidine (Scheme 1). Conditions were optimized to increase the ratio between the desired mono derivative (**6**) and the disubstituted product (**5**). Initially we experimented with the conditions employed for the synthesis of three-side-chained DAPER derivatives[12] treating **4** with piperidine at room temperature. We obtained **6** almost in equal amount with respect to the disubstituted product **5**. After experimenting with several reaction conditions (see Table S2 in the Supporting Information), we obtained better results at higher temperatures, as described in the Experimental Section. We also tried to add hydroquinone to the reaction mixture, which is a molecule able to capture radicals. In fact, in our experience, when hydroquinone is added to different reactions to avoid the formation of dehalogenated products, it seems to be able to delay the displacement of the second bromine atom; an observation that could suggest the involvement of a radicalic mechanism (data not shown). To optimize the reaction conditions we tried also to use an excess of piperidine and the reaction was stirred at 100 °C for a shorter time. We also compared the reaction yields in the absence and presence of hydroquinone, identifying the latter conditions as optimal. The products obtained by this reaction are not easily and completely separable by column chromatography, so the partially purified mixture was used in the following synthetic step. The relative ratio values of compounds **5**/**6** were calculated from the ^{1}H NMR spectra.

To proceed towards the extension of the aromatic core, a suitable functionalized alkyne (**7**) was prepared, having 1-piperidine at the end of the linear chain.[11] This alkyne was successively used in a Sonogashira cross-coupling[13] to synthesize the intermediate compound **8**. This reaction is catalyzed by Pd^0 complexes in the presence of Cu^I and a suitable base, leading to a new C–C bond. In contrast to the previously reported synthesis of coronene derivatives, in this case the Sonogashira reaction conditions led to the asymmetrical compound **8** due to the presence of only one bromine atom on compound **6**. In

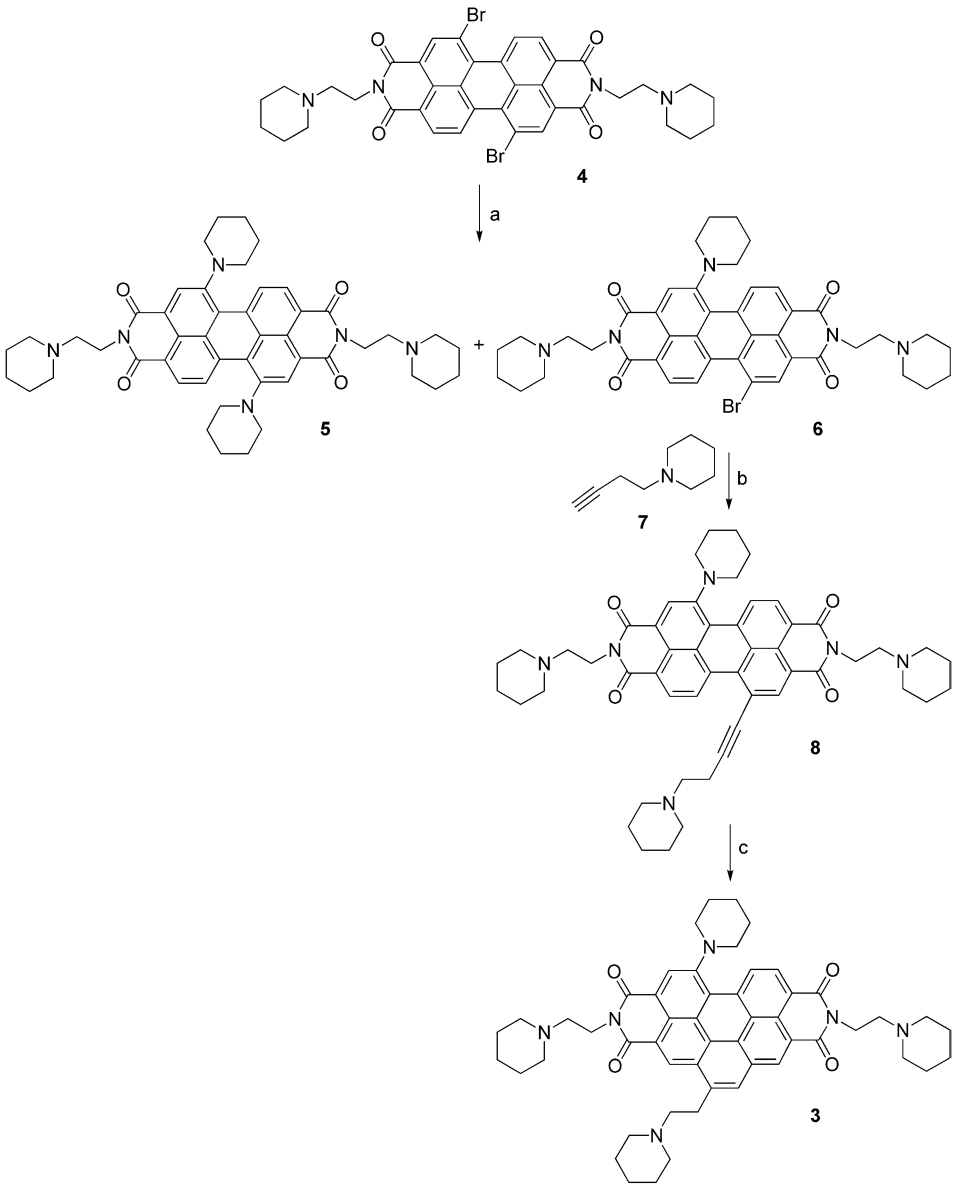

Scheme 1. *Reagents and conditions*: a) Hydroquinone, piperidine, anhydrous dioxane, 100 °C, argon atmosphere, 40 min; b) THF, Et_3N, CuI, $[Pd(PPh_3)_4]$, argon atmosphere, 80 °C, 20 h: c) DBU, toluene, argon atmosphere, heated to reflux, 20 h.

the Sonogashira coupling, the cyclization described in the next step also partially occurs. Separation was not useful at this stage, so the mixtures were used in the following step. To complete the aromatic core, a base-catalyzed cyclization was performed with 1,8-diazabicyclo-[5.4.0]undec-7-ene (DBU). In this way the desired compound **3** was obtained (Scheme 1), which was converted into the respective water-soluble hydrochloride by precipitation with diethyl ether from an acidic (HCl) methanol solution.

ESI-MS study of binding affinity and selectivity

The new synthesized derivative **3** was studied by ESI-MS to evaluate its ability to bind the intramolecular quadruplex structure formed by the human telomeric sequence and its selectivity with respect to duplex DNA.[10] To this aim, an oligonucleotide representing four human telomeric repeats (21-TT, 5′-GGGTTAGGGTTAGGGTTAGGGTT-3′) and a model oligonucleotide for duplex DNA (DK66, 5′-CGTAAATTTACG-3′) were used. The association constants K_1 and K_2, relating to the equilibrium for the formation of drug–DNA complexes with 1:1 and 2:1 stoichiometry respectively, as well as the corresponding percentage of bound DNA, are reported in Table 1, with the relative standard deviations.

The collected data demonstrates that **3** is a stronger G4 ligand than the previously reported coronene derivative **2**,[10d] showing a K_1 value substantially equal to **2** but a K_2 value that is two orders of magnitude higher. In fact, calculating the total amount of ligand bound in the 1:1 ratio experiments, the values obtained were higher than 99%, showing full saturation. Compound **3** displayed a low affinity towards duplex oligonucleotide by binding twice as much quadruplex DNA as duplex DNA, showing enhanced selectivity compared to **2**.[10d] On the other hand, this selectivity is lower than that showed by previously reported **1**, even though compound **3** has a much higher G4-binding ability. So we decided to perform competition experiments by using genomic DNA from calf thymus (CT).[8] Due to the high affinity demonstrated to-

Table 1. Values of Log K_1 and Log K_2 and bound DNA (%).[a]

	21-TT			DK66		
	Log K_1	Log K_2	Bound DNA [%]	Log K_1	Log K_2	Bound DNA [%]
PPL3C[8] (**1**)	5.8 ± 0.2	5.0 ± 0.1	56 ± 7	3.9 ± 0.2	4.2 ± 0.1	< 5
CORON[10d] (**2**)	6.6 ± 0.3	4.2 ± 0.1	78 ± 5	6.0 ± 0.3	5.2 ± 0.2	59 ± 5
EMICORON (**3**)	6.5 ± 0.2	6.3 ± 0.2	73 ± 2	5.4 ± 0.1	4.9 ± 0.1	38 ± 1

[a] K_1 and K_2 values (reported on a logarithmic scale) and percentage of bound DNA calculated at 1:1 drug/DNA ratio, as described in the Experimental section, for the indicated oligonucleotides. Values represent the mean ± standard deviation (SD) of at least three independent experiments.

wards the G4 structure, it was possible to perform these experiments with a lower drug concentration. At half the concentration of drug and DNA both the 1:1 and the 2:1 complexes were clearly visible (see Figure S2 in the Supporting Information). Percentages of bound DNA in the absence and in the presence of calf thymus DNA are reported in Table 2.

Compound **3** showed a good selectivity in competition experiments, similar to **1**[8] and **2**[10d] toward the same oligonucleotide (which is the biologically relevant human telomeric sequence), but with the advantage of an increased binding affinity. In fact, it is worth noting that the results shown have been obtained at a 0.5 drug/DNA ratio, whereas in the other cases 1:1 experiments were performed due to the minor binding affinity of the drug.

Table 2. Competition experiments on the 21-TT oligonucleotide.[a]

	21-TT/CT DNA ratio				
	no CT	1:1	*N*[%] at 1:1	1:5	*N*[%] at 1:5
PPL3C[8] (**1**)	56±7	47±3	0.84	39±1	0.70
CORON[10d] (**2**)	78±5	63±5	0.81	42±5	0.54
EMICORON (**3**)[b]	38±1	33±1	0.87	22±1	0.58

[a] Values of percentage of bound 21-TT and normalized percentage bound quadruplex ($0<N\%<1$), as defined in the Experimental Section, for samples containing a fixed amount of both drug and G4 DNA and different amounts of calf thymus DNA (CT), at the indicated quadruplex/duplex ratios (in phosphate ions). Values represent the mean ± SD of at least three independent experiments. [b] Data obtained at a drug/DNA ratio of 0.5:1.

Effect on the telomerase/telomere pathway

Due to the inability of telomerase to extend a quadruplex-folded telomeric substrate, G4 ligands were firstly designed as telomerase inhibitors. We therefore investigated the ability of **3** to inhibit human telomerase activity in a cell-free system by means of a telomerase repeat amplification protocol (TRAP) assay. Of note, although a major risk of handling variability exists, to avoid false-positive results and/or overestimate the inhibitory effect of the G4 ligand, the TRAP assay has been performed by removing the inhibitor after telomerase extension.[14] This is an important step during the PCR-based TRAP assay because most G4 ligands can interfere with the PCR amplification of a sequence able to form a G4. As it is evident from the Figure 2, compound **3** was able to inhibit telomerase activity in a dose-dependent manner. However, this effect occurred at a very high dose of the drug; the IC_{50} value is approximately 30 μM under the experimental conditions and therefore **3** is a poor telomerase inhibitor.

Consequently, the ability of **3** to cause telomere uncapping has been investigated (Figure 3). To this aim, a two-step analysis was performed to establish, firstly, if the compound was able to induce DNA damage and, secondly, if this DNA damage was localized to the telomeres. In particular, BJ fibroblasts (human foreskin) expressing human telomerase reverse transcriptase (BJ-hTERT) or hTERT and SV40 early region (BJ-HELT), were exposed to different drug concentrations for 12 h. The results demonstrated that **3** was able to induce DNA damage, as revealed by the increased percentage of both γH2AX- and 53BP1-positive cells and this effect was selective for transformed cells (Figure 3a). Indeed, γH2AX and 53BPI were not significantly ($P>0.05$) activated in normal telomerized fibroblasts upon treatment with **3**, even at the highest drug concentration (Figure 3a). The selective DNA damage induced by **3** in transformed cells prompted further studies to investigate the telomere specific effects of this ligand. Deconvolution microscopy analysis, reported in Figure 3b, revealed that some of the damaged foci (both γH2AX and 53BP1) induced by **3** co-localized with TRF1, a good marker for interphase telomeres[15] forming the so-called TIFs (telomere-dysfunction induced foci).[16] Quantitative analysis revealed that treatment with **3** significantly ($P<0.01$) increased the percentage of cells with more than four γH2AX/TRF1 co-localizations (the percentage of TIFs-positive cells reached about 50% upon treatment with 0.1 μM concentration), with a mean of about seven TIFs per nucleus (Figure 3c).

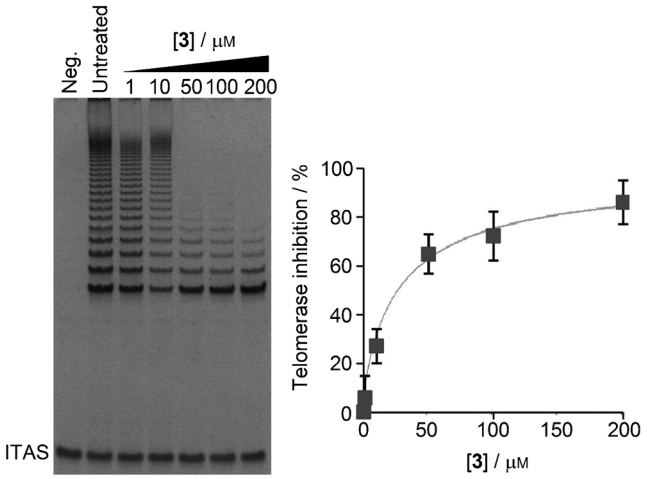

Figure 2. Inhibition of telomerase activity. Telomerase activity was evaluated by the telomerase repeat amplification protocol (TRAP) assay as reported in the Experimental Section. Compound **3** was added at different concentrations ranging from 1 to 200 μM. Before PCR, the samples were purified by phenol/chloroform extraction. Products were resolved on 12% PAGE and visualized with SYBR Green staining. A representative TRAP assay is showed. The quantitative analysis was undertaken as reported in the Experimental Section, and data represent the mean of three independent experiments with similar results. The intensities of TRAP products were normalized to the intensities of the corresponding bands in the untreated sample. Telomerase inhibition (%) was plotted against compound concentration to determine the IC_{50} value ($IC_{50}=27.0\pm2.0$ μM).

To determine the cause of telomere uncapping, we investigated the localization of TRF1, telomeric repeat binding factor 2 (TRF2), and protection of telomeres 1 (POT1), three telomeric proteins inducing telomere dysfunction and evoking a DNA damage signal when their levels are reduced at telomeres. A ChIP assay showed that **3** delocalized POT1 from telomeres, whereas TRF1 and TRF2 remained associated to the telomeres upon treatment with the ligand (Figure 3d).

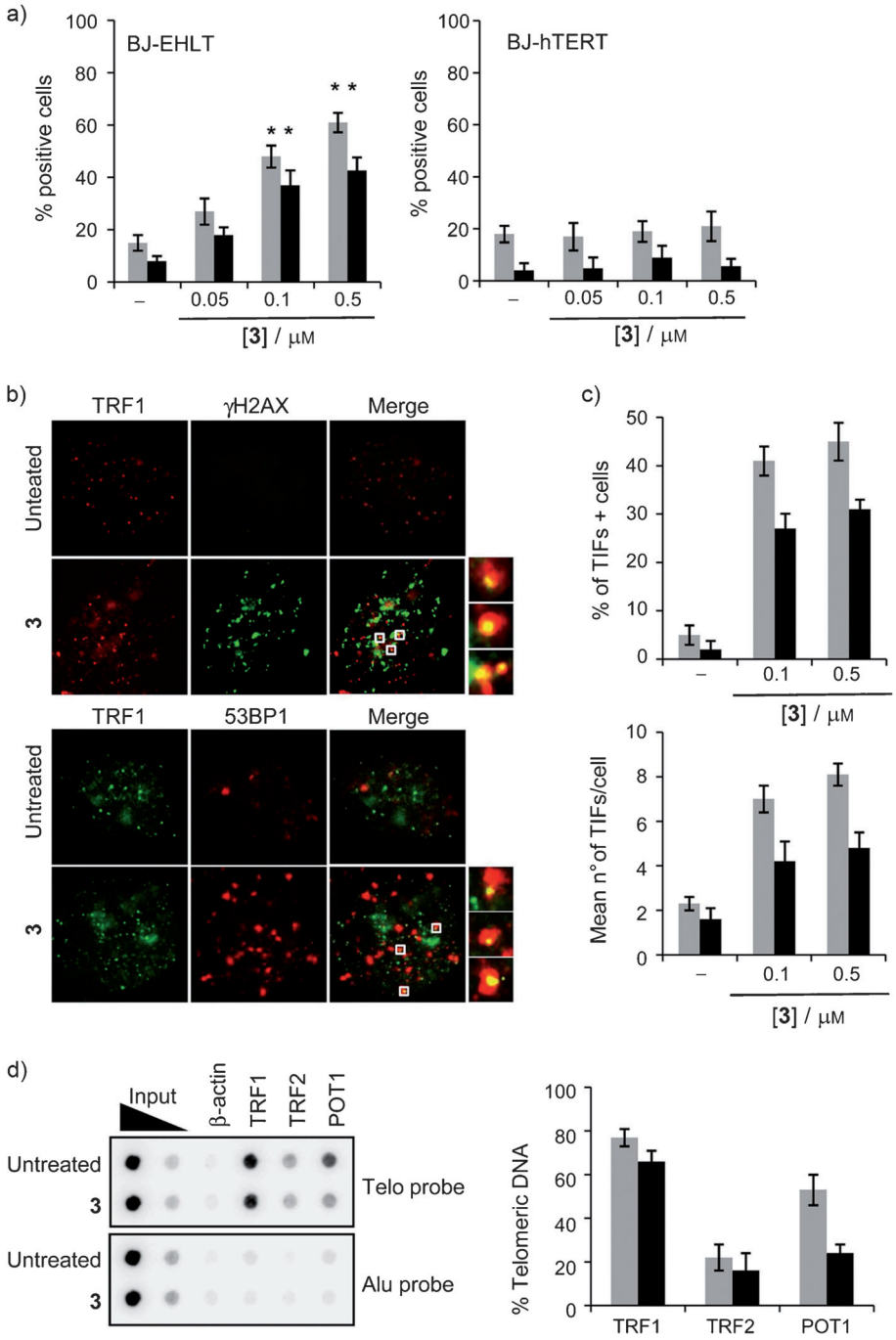

Figure 3. Activation of DNA damage response in transformed cells is associated with the displacement of POT1 from telomeres. a) Transformed (BJ-EHLT) and normal telomerized (BJ-hTERT) human fibroblasts were treated with different concentrations of **3** for 24 h, fixed, and processed for IF by using antibodies against γH2AX and 53PB1. Quantitative analysis, showing the percentage of γH2AX-(gray bars) and 53PB1-positive cells (black bars), is reported. Three independent experiments were performed, and error bars indicate the standard deviation (SD); [**] = ($p < 0.01$). b) Untreated and **3**-treated BJ-EHLT cells were co-immunostained with antibodies against TRF1 and γH2AX or 53BP1 and processed for IF. Representative images of IF were acquired with a Leica Deconvolution microscope (magnification 100×). Enlarged views are reported on the right of the merged images from **3**-treated samples. c) Percentage of TIFs-positive cells and average number of TIFs per nucleus in untreated treated cells. Cells with four or more γH2AX (gray bars) or 53BP1/TRF1 foci (black bars) were scored as TIFs-positive. The mean of three independent experiments with similar results is reported. Error bars indicate the SD. D) Chromatin extracts from the indicated samples were subjected to ChIP analysis using antibodies against TRF1, TRF2, and POT1. A β-actin antibody was used as the negative control. The total DNA (input) represents 10 and 1% of genomic DNA. Southern blot analysis was performed by using telomeric (Telo) or ALU repeat-specific probes. A representative experiment is shown on the left panel. The signals obtained were quantified by densitometry, and the percentage of precipitated DNA for each untreated (gray bars) or compound **3**-exposed (black bars) sample was calculated as a ratio of input signals and plotted in the graph (right panel). Four independent experiments were performed, and error bars indicate the SDs.

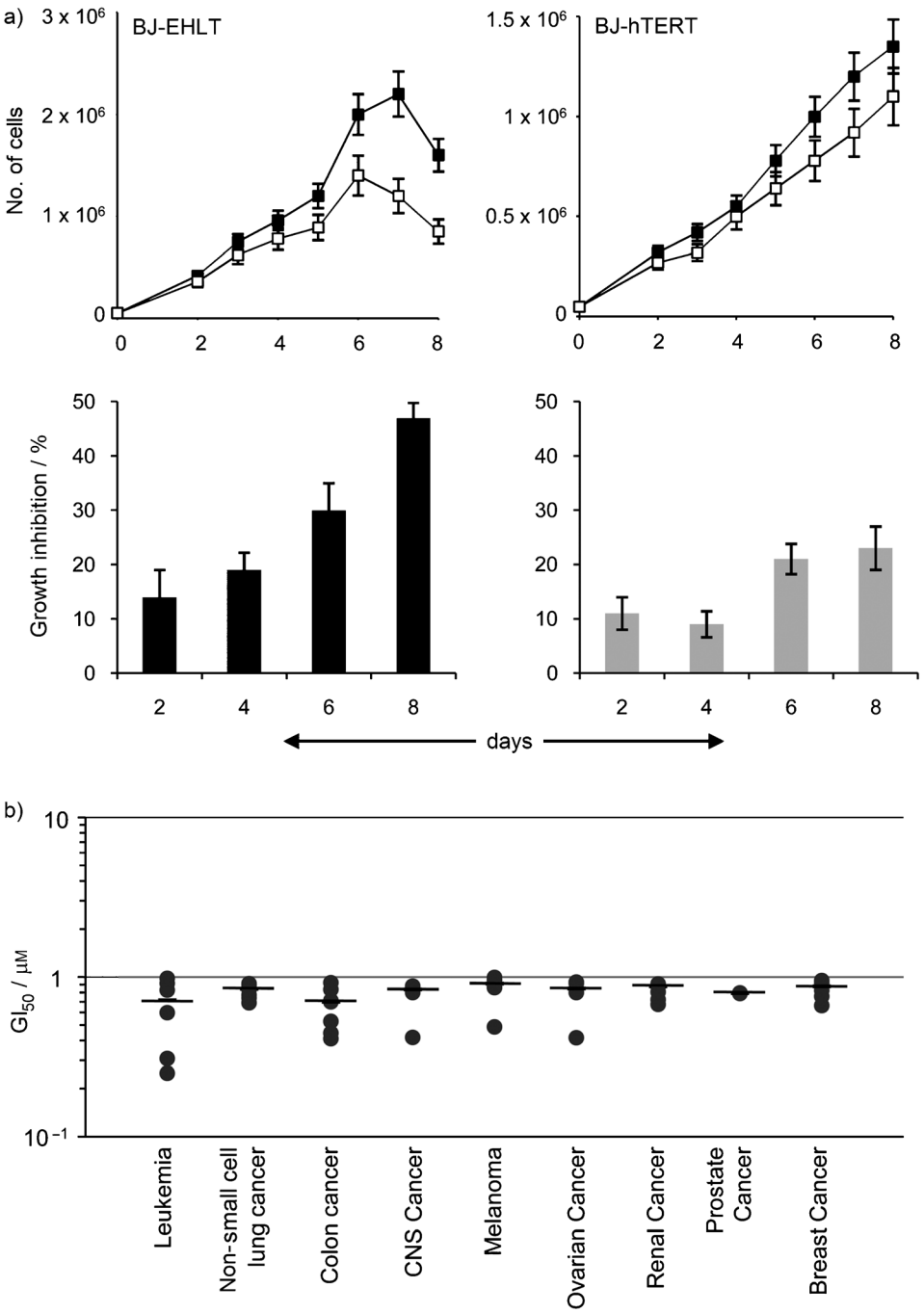

Figure 4. Antiproliferative effect of compound **3** is specific for transformed and tumor cells. a) Upper panels: in vitro growth curves of BJ-EHLT and BJ-hTERT untreated (■) and treated (□) with **3** (0.1 μM). The figures show representative experiments performed in quintuplicate with SDs. Lower panels: percentage of growth inhibition of drug-treated versus untreated cells calculated at day 2, 4, 6, and 8 of cell culture. b) Cytotoxicity of **3** in the NCI in vitro 60 human cancer cell lines drug screen program.

Effect on cellular proliferation and tumor survival

Telomeres emerge as cellular integrators of various stresses.[17] Consequently, changes in their structure profoundly affect the ability of cells to proliferate and to adapt to a new environment. Notably, even if the molecular mechanism(s) were not yet described, pharmacological telomere damage induced by G4 ligands triggers a selective anticancer effect on transformed and tumor cells. Therefore, the above results raise the interesting possibility that telomere damages induced by **3** may rapidly promote growth inhibition selectively in malignant cells. Transformed- and normal telomerized fibroblasts were exposed to the lower dose of drug able to trigger telomere damage when cells were exposed for 12 h. The growth curves of untreated and drug-treated cells were analyzed from 2 to 8 days of culture (Figure 4a). A significant time-dependent decrease of cell proliferation has been observed in transformed BJ-EHLT cells treated with the ligand, reaching the maximum effect at day 8. Interestingly, at the same drug dose, compound **3** slightly reduces the cell proliferation of normal telomerized fibroblasts (being the growth inhibition about 20% at days 6–8 of culture), suggesting that this agent would preferentially kill cancer cells.

On the basis of these results, compound **3** was studied for antiproliferative activity against human cancer cell lines by the US National Cancer Institute (NCI)/National Institutes of Health (NIH) developmental therapeutics program.[18] In particular, this compound has been evaluated in the full panel of human tumor cell lines derived from nine cancer cell types (leukemia, melanoma and cancers of non-small cell lung, colon, CNS, prostate, ovarian, renal, and breast). Figure 4b shows the GI_{50} (dose inhibiting the 50% of the tumor growth) of each cell line by subpanel group; the full data are reported in the Supporting Information (Table S3). Evidently, compound **3** is highly active in inhibiting tumor cell proliferation; the GI_{50} median value of each cell line from the subpanel groups was shown to be less than 1 μM (Figure 4b).

The effect of **3** on tumor cells has been also evaluated by clonogenic assay both in telomerase-negative and -positive tumor cells. In particular, the analysis was performed on U2OS cells, which maintain telomeres through alternative mechanism (ALT) and on three telomerase-positive cell lines of different

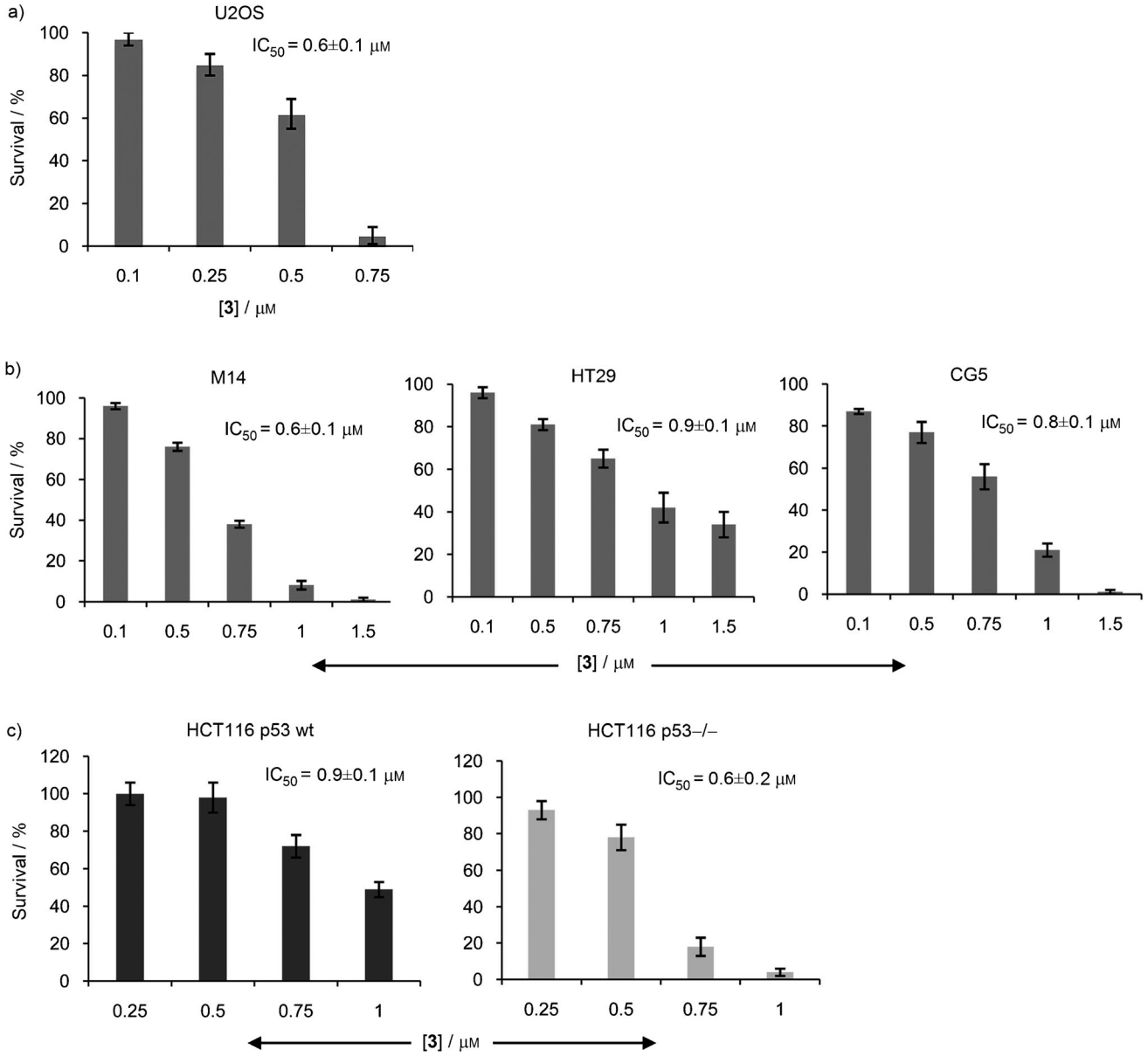

Figure 5. Cytotoxic activity of compound **3** in different tumor cell lines: a) Human U2OS osteosarcoma, M14 melanoma; b) HT29 colorectal adenocarcinoma, CG5 breast cancer cell lines, and c) wild-type or p53-deficient HCT116 colon cancer cell lines were treated with the indicated doses (ranging from 0.1 to 1.5 μM) of compound **3** for 96 h and the colony-forming ability was evaluated as reported in the Experimental Section. Surviving fractions were calculated as the ratio of absolute survival of the treated sample/absolute survival of the control sample. Three independent experiments were performed, and error bars indicate the SDs.

histotype, M14 melanoma, HT29 colon and CG5 breast carcinomas. The results, reported in Figure 5, show that **3** inhibited cell survival in a dose-dependent manner in all the tumor lines employed, regardless the presence of telomerase, and more interestingly, the IC_{50} values being always below to 1 μM (Figure 5a). More interestingly, even if **3** was active both in tumor cells expressing the wild type or mutant p53, the lack of this oncosuppressor in the HCT116 colon-carcinoma cell line, can make the cells more sensitive to treatment with **3**, the IC_{50} value being reduced up to about 40% in p53-/- compared to the wild-type cells.

Discussion and Conclusions

Our previous results on N-cyclic bay-substituted perylene diimides showed that one piperidinyl group is necessary to ensure quadruplex-versus-duplex selectivity; the second group cannot bring any further advantage, making the interaction with the ending tetrad of the quadruplex structure more difficult.[8]

Herein we have designed the "chimera" molecule **3**, having one piperidinyl group bound to the perylene bay area and an extended aromatic, describing the synthesis of this new asymmetric compound. Initially, by using ESI-MS, we studied the

binding of this compound to the human telomeric G-rich sequence and its selectivity with respect to duplex DNA, also in the case of genomic DNA. We found that **3** shows a good quadruplex-versus-duplex selectivity, but with the advantage of higher binding constants than the previously reported compounds, both with respect to N-cyclic bay-monosubstituted perylene diimide **1** and to coronene derivative **2**.

From a molecular point of view, compound **3** inhibits telomerase activity, even if this effect occurs at very high drug concentration. However, it is difficult to compare the IC_{50} value of this compound with that of other G4 ligands available in the literature because, as already noted in several papers, the IC_{50} value derived from the TRAP assay depends on the assay conditions and primer concentration.[6b,19,20] More importantly, many studies have used the TRAP assay without removing the inhibitor prior to the PCR step. As a consequence, the inhibitory effect of many G4 ligands has been overestimated. However, since the biological effects were also quickly observed in telomerase-negative ALT cells, we can conclude that the impairment of telomere elongation by **3** is not the main mechanism of drug action.

Considering that (from a biological point of view) compound **3** cannot be considered a telomerase inhibitor, we still decided to proceed in the analysis of its molecular and biological effects. This decision was based on data demonstrating that the presence of telomerase in tumor cells (as a mechanism of telomere maintenance), is not mandatory for the antitumoral activity of G4-interactive compounds.[6–8,20] Thus, we looked beyond telomerase activity and function and we focused on the capped status to evaluate telomere functionality following treatment with the telomere-targeting agent. Our results clearly demonstrated that **3** rapidly disrupts the telomere architecture of cells resulting in a potent DNA damage response characterized by the formation of several telomeric foci containing phosphorylated H2AX and 53BP1, which are two of the main hallmarks of DNA double-strand break. This is typical of the telomere deprotection occurring during cellular senescence or upon the loss of telomeric proteins.[15,21] Consistently, compound **3** specifically delocalizes POT1 from telomeres, whereas both TRF1 and TRF2 remain associated to the TTAGGG repeats. Of note, compound **3** is more potent than the previously described **1** in inducing telomere damage and (in agreement with these results) it is able to limit the growth of transformed cells at a 5-times-lower drug concentration. The ability of G4 ligands to uncap telomeres and to possess antitumoral activity has been already described for other agents,[6,7,22] reinforcing the notion that these agents can act as inhibitors of telomere-related process and therefore the rationale for the development of this class of inhibitors as antitumoral agents must be found elsewhere other than in higher telomerase expression in cancer cells.

Since telomere is not a selective target for transformed and tumor cells, the telomere damage and antiproliferative activity of **3** has been evaluated on normal and transformed cells, with the aim to verify if this new chimera molecule can maintain the telomere specificity of the previous reported **1**.[8] The results clearly demonstrated that telomere damage and antiproliferative activity induced by **3** is clearly evident in transformed cells, whereas normal telomerized fibroblasts are only weakly affected by the treatment. This result strongly suggests that this agent displays a marked narrow window for selectivity, which presents an interesting situation in the light of the future clinical development of this new class of antitumoral drugs. These findings are in good agreement with the quadruplex-versus-duplex selectivity derived by ESI-MS, as well as with the stronger G4 binding ability of this compound with respect to the previously reported compounds of these series. This enforces the idea that ESI-MS can be a quick and efficient method to screen G4 ligands and to predict their activity.

The interestingly activity on transformed fibroblasts has been also observed on cancer cells as reported by the data from the NCI Drug Screen Program. Indeed, compound **3** is highly active on all the human tumor cell lines tested; the GI_{50} values being always below the 1 μM concentration, regardless the tumor hystotype, thus providing a compelling rationale to target telomere pathway for broad-spectrum cancer therapy. Again, these results have been corroborated by using the clonogenic assay, which is considered the most valid in vitro test to measure the surviving fraction of cells after a drug treatment, and are consistent with a cancer stem cell targeting mechanism. Finally, the efficacy of **3** on all the transformed and tumor cell lines tested, suggests that the oncosuppressor p53, one of the main apoptosis inducers that is frequently mutated on cancers, is not necessary for the response of tumor cells to the G4 ligand. However, the use of a genetically-defined tumor model of HCT116 colon carcinoma cell line, possessing the wild-type or mutant p53 in the same genetic background, revealed that the lack of this oncosuppressor can make the cells more sensitive to the treatment with **3**. Taken together, these results indicate that p53 can be involved in the repair of G4-induced telomere damage rather than in tumor cell death.

In conclusion, in this paper we have identified the chimera molecule **3** as a new promising G4 ligand having a strong antitumoral effect, typical of the hydrosoluble coronene derivatives, and an intriguing selectivity toward tumor cells, characteristic of the perylene derivatives, providing a compelling argument to suggest that telomere is a well-validated target at the preclinical level.

Experimental Section

Chemistry

General: All commercial reagents and solvents were purchased from Fluka and Sigma–Aldrich, and used without further purification. TLC glass plates (silica gel 60 F_{254}) and silica gel 60 (0.040–0.063 mm) were purchased from Merck. ^1H and ^{13}C NMR spectra were performed with Varian Gemini 200 and Varian Mercury 300 instruments. ESI-MS spectra were recorded on a Micromass Q-TOF MICRO spectrometer. Starting compounds **4** and **7** were prepared as previously described[11] (for details, see the Supporting Information). All compounds used in the biophysical and biological evaluations were >95% pure as determined by HPLC (instrument: HPLC-

Waters 2487; column: SUPELCO LC-Diol HPLC Column, 5 μm particle size, L×I.D. 25 cm×4.6 mm).

***N,N′*-Bis[2-(1-piperidino)-ethyl]-1-(1-piperidinyl)-7-bromoperylene-3,4:9,10-tetracarboxylic diimide (6)**: Compound **4** (50 mg, 64.93 μmol; actually a mixture of the two possible isomers; for details, see the Supporting Information) and hydroquinone (25 mg, 227.27 μmol) were stirred in piperidine (2 mL) and anhydrous dioxane (2 mL) at 100 °C under argon for 40 min. After cooling, water was added (20 mL), and the crude product was extracted with $CHCl_3$ (3×50 mL). The organic layer was extracted with water until the aqueous layer was neutral. After drying over Na_2SO_4, filtering, and concentration in vacuo, the crude product was purified by column chromatography on a silica gel ($CHCl_3$/MeOH 98:2). The complete separation of **5** and **6** was not possible; the fractions obtained by chromatography showing a suitable aromatic pattern in the ^{1}H NMR spectra (as reported below) were collected, and the mixture was used in the subsequent step. ^{1}H NMR (200 MHz, $CDCl_3$): δ = 9.27 (d, J = 8 Hz, 1H, aromatic H), 9.22 (d, J = 8 Hz, 1H, aromatic H), 8.66 (s, 1H, aromatic H), 8.36 (s, 1H, aromatic H), 8.52 (d, J = 8 Hz, 1H, aromatic H), 8.40 (d, J = 8 Hz, 1H, aromatic H), 4.59 (m, 4H, N_{imidic}-CH_2), 3.37 (m, 2H, C_{ar}-$N_{piperidine}$-CH_2), 2.95 (m, 2H, C_{ar}-$N_{piperidine}$-CH_2), 3.11 (broad, 12H, $N_{piperidine}$-CH_2), 1.93 (broad, 8H, $N_{piperidine}$-CH_2-C*H*$_2$), 1.73 (m, 4H, C_{ar}-$N_{piperidine}$-CH_2-C*H*$_2$), 1.62 (broad, 4H, $N_{piperidine}$-CH_2-CH_2-C*H*$_2$), 1.48 ppm (broad, 2H, C_{ar}-$N_{piperidine}$-CH_2-CH_2-C*H*$_2$).

***N,N′*-Bis[2-(1-piperidino)-ethyl]-1-(1-piperidinyl)-7-[3-(1-piperidino)-butinyl]-perylene-3,4:9,10-tetracarboxylic diimide (8)**: PP_3CBr **6** (2.5 g, 3.23 mmol; mixture of mono and disubstituted derivatives: see above), was dissolved in anhydrous THF (40 mL) and Et_3N (40 mL); then CuI (61 mg, 0.32 mmol) and [$Pd(PPh_3)_4$] (367 mg, 0.32 mmol) were added. After bubbling argon through the solution, the reaction mixture was heated at 80 °C with stirring and 1-(3-butynyl)-piperidine **7** (829 mg) was added dropwise. The mixture was then stirred at 80 °C overnight in an argon atmosphere. After cooling, dilute HCl (10 mL) was added and, after neutralization with 2 M aq NaOH, the product was extracted with CH_2Cl_2 (3×50 mL). The organic layer was washed with water until the aqueous layer was neutral. After treatment with anhydrous Na_2SO_4 and filtration, the solvents were evaporated under vacuum. Since partial cyclization can occur at this stage, complete separation of the different products and a full characterization were not possible so the crude product (3 g) was used in the following cyclization step without further purification.

***N,N′*-Bis[2-(1-piperidino)-ethyl]-1-(1-piperidinyl)-6-[2-(1-piperidino)-ethyl]-benzo[ghi]perylene-3,4:9,10-tetracarboxylic diimide (3, EMICORON)**: Toluene (100 mL) and 1,8-diazabicyclo[5.4.0]undec-7-ene (DBU) (1.66 mL) were added to the intermediate compound **8** (2.7 g, 3.25 mmol) and the reaction mixture was heated to reflux with stirring under argon for 20 h. After cooling, CH_2Cl_2 (100 mL) was added, and the organic layer was extracted with water until the aqueous layer was neutral. The crude product was purified by column chromatography on silica gel ($CHCl_3$/MeOH 100:0, 98:2, 95:5, 90:10, 80:20, and 70:30) to give 1.5 g (55% yield) of the desired compound. The product was then crystallized by dissolving in a mixture of MeOH and 37% aq HCl solution (95:5) and precipitating the respective hydrochloride with diethyl ether. From this crystallization, 350 mg of hydrochloride salt was obtained from 420 mg of basic compound (71% yield). ^{1}H NMR (300 MHz, $CDCl_3$): δ = 10.30 (d, J = 8.7 Hz, 1H, aromatic H), 9.11 (s, 1H, aromatic H), 8.91 (s, 1H, aromatic H), 8.60 (d, J = 8.7 Hz, 1H, aromatic H), 8.55 (s, 1H, aromatic H), 8.26 (s, 1H, aromatic H), 4.51 (m, 4H, N_{imidic}-CH_2), 3.70 (broad, 2H, C_{ar}-CH_2), 3.34 (broad, 2H, C_{ar}-$N_{piperidine}$-CH_2), 2.94 (broad, 2H, C_{ar}-$N_{piperidine}$-CH_2), 2.84 (broad, 18H, $N_{piperidine}$-CH), 1.69 ppm (broad, 24H, $CH_{piperidine}$); ^{13}C NMR (300 MHz, $CDCl_3$): δ = 163.8 (C=O), 163.7 (C=O), 163.6 (C=O), 163.5 (C=O), 152.8 (C_{ar}), 138.7 (C_{ar}), 133.1 (C_{ar}), 132.4 (C_{ar}), 129.0 (C_{ar}), 128.9 (C_{ar}), 128.4 (C_{ar}), 127.2 (C_{ar}), 126.7 (C_{ar}), 126.1 (C_{ar}), 125.6 (C_{ar}), 125.0 (C_{ar}), 124.9 (C_{ar}), 123.3 (C_{ar}), 123.0 (C_{ar}), 122.9 (C_{ar}), 121.9 (C_{ar}), 121.7 (C_{ar}), 121.6 (C_{ar}), 121.2 (C_{ar}), 120.2 (C_{ar}), 60.3, 56.3, 54.8, 54.7, 54.6, 53.4, 37.9, 37.7, 30.8, 26.0, 25.9, 24.4, 24.3, 23.8 ppm; MS (ESI): *m/z*: calcd for $C_{52}H_{59}N_6O_4$: 831.4598 [$M+H^+$]; found: 831.4580.

Electrospray ionization mass spectrometry (ESI-MS)

Complexes formed between ligands and quadruplex/duplex DNA were determined by using ESI-MS. Single-stranded oligonucleotides were purchased from Eurofins MWG Operon (Ebersberg, Germany) with the following sequences: 5′-GGGTTAGGGTTAGGGTTAGGGTT-3′ (21-TT) and 5′-CGTAAATTTACG-3′ (DK66). ESI-MS spectra were recorded on a Micromass Q-TOF MICRO spectrometer (now Waters) in the negative ionization mode. The rate of sample infusion into the mass spectrometer was 5 μL min^{-1} and the capillary voltage was set to −2.6 kV. The source temperature was adjusted to 70 °C, the cone voltage to 30 V, and the collision energy to 5 V. Data were analyzed by using the MassLynx software developed by Waters. Samples were prepared by mixing appropriate volumes of ammonium acetate buffer (150 mM), annealed oligonucleotide stock solution (50 μM), stock solutions of **3** (100 μM), and methanol. The final concentration of DNA in each sample was 5 μM (in duplex or quadruplex unit) and the final volume of the sample was 50 μL. After the binding equilibrium in ammonium acetate was established, methanol (as 15% w/v) was added to the mixture just before injection to obtain a stable electrospray signal. As a reference, samples containing only 5 μM DNA with no drug were prepared. Samples for competition experiments were prepared following the procedure described above, adding an appropriate volume of CT DNA solution. Final concentrations of quadruplex DNA and drug solutions were always 5 μM and CT was added at two different duplex/quadruplex ratios (1 and 5), calculated on the basis of phosphate group concentrations. To minimize random errors, each experiment has been repeated at least three times under the same experimental conditions. Data were processed and averaged with the SIGMA-PLOT software.

For drug–DNA complexes with 1:1 and 2:1 stoichiometry, which have been shown to be the main species present in solution in all the experiments, the formation of such complexes can be represented by two distinct equilibrium, which are described by the following two equations: K_1 = [1:1]/([DNA] [drug]) and K_2 = [2:1]/([1:1] [drug]), in which [DNA], [drug], [1:1] and [2:1] represent respectively the concentrations of the different species in solution: DNA (duplex or quadruplex depending on the oligonucleotide used), the ligand, the 1:1 and 2:1 drug–DNA complexes at equilibrium. The association constants K_1 and K_2 can be calculated directly from the relative intensities of the corresponding peaks found in the mass spectra, with the assumption that the response factors of the oligonucleotides alone and of the drug–DNA complexes are the same, so that the relative intensities in the spectrum are supposed to be proportional to the relative concentrations in the injected solution.[10] The percentage of bound DNA was calculated according to an equation developed by Brodbelt and co-workers,[10] which represents the percentage of DNA bound ligand: Bound DNA (%) = 100([1:1] + [2:1])/([DNA] + [1:1] + [2:1]). To elaborate the data obtained in the competition experiments, this percentage has been normalized with respect to the same percentage obtained in the presence and in the absence of calf thymus DNA, according to

the formula: $N(\%) =$ quadruplex bound in presence of CT (%)/ quadruplex bound in absence of CT (%).

Biological evaluation

Cells and culture conditions: BJ fibroblasts expressing hTERT (BJ-hTERT) or hTERT and SV40 early region (BJ-HELT), M14 melanoma, HT29 colon and CG5 breast carcinomas were obtained as previously reported.[7a] Human U2OS osteosarcoma and HCT116 colorectal carcinoma cell lines were obtained from ATCC; HCT116 p53-/- cells were a generous gifts from Bert Vogelstein at Johns Hopkins Medical Institutions, Baltimore, MD, USA. All the lines were grown in Dulbecco's Modified Eagle Medium (DMEM, Invitrogen Carlsbad, CA, USA) supplemented with 10% fetal calf serum, 2 mM L-glutamine and antibiotics.

Immunofluorescence: Immunofluorescence was performed as previously reported.[7a] Cells were fixed in 2% formaldehyde and permeabilized in 0.25% Triton X100 in PBS for 5 min at room temperature. For immunolabeling experiments, cells were incubated with primary antibody, then washed in PBS and incubated with the secondary antibodies. The following primary antibodies were used: pAb and mAb anti-TRF1 (Abcam Ltd.; Cambridge UK); mAb anti-γH2AX (Upstate, Lake Placid, NY), and pAb anti-53BP1 (Novus Biologicals Inc., Littleton, CO). The following secondary antibodies were used: TRITC-conjugated goat anti-rabbit and FITC-conjugated goat anti-mouse (Jackson Lab.). Fluorescence signals were recorded by using a Leica DMIRE2 microscope equipped with a Leica DFC 350FX camera and elaborated by Leica FW4000 deconvolution software (Leica, Solms, Germany).

Chromatin Immunoprecipitation assay (ChIP): BJ-HELT fibroblasts were treated for 72 h with 0.5 μM of compound **3**. The ChIP assay was performed as previously described.[7a] The following antibodies were used: pAb anti-TRF1 (Santa Cruz Biotechnology, Santa Cruz, Ca); mAb anti-TRF2 (Imgenex, San Diego, CA); pAb anti-POT1- (Abcam); mAb anti-β-actin (Sigma, Chemicals, Milano, Italy) was used as a negative control in the ChIP assay.

TRAP assay: Telomerase enzyme activity was measured with the PCR-based TRAP kit (Chemicon International, MA, USA), as previously reported.[23] Before the PCR step, to purify the elongated products and remove the bound ligand, extraction with phenol/chloroform/isoamyl-alcohol (50:49:1) was performed and DNA was precipitated over night at $-20\,^{\circ}C$. Reaction products were amplified in the presence of a 36 bp ITAS and each set of TRAP assay included a control reaction without extract (negative control). Samples were separated on 12% PAGE and visualized with SYBR Green staining (Sigma–Aldrich). Gels were quantified using a gel scanner. The intensity data were obtained by scanning and integrating the total signal of each PCR product ladder in the denaturing gels. Drug samples were corrected for background by subtracting the fluorescence reading of negative controls. The data was collected at a range of concentrations to obtain dose-response curves from with the IC_{50} values (the concentration required for 50% enzyme inhibition) were obtained.

Cytotoxic assays: Cell growth was assessed by seeding 5×10^4 cells in 60 mm Petri plates (Nunc, MasciaBrunelli, Milano, Italy) and 24 h after plating, freshly dissolved **3** (0.1 μM) was added to the culture medium. Cell counts (Coulter Counter, Kontron Instruments, Milano, Italy) and viability (trypan blue dye exclusion) were determined daily, from day 1 to day 8 of culture. To evaluate the cell colony-forming ability, cells were seeded at a density of 2×10^5 cells per 60 mm dish and exposed for 96 h to different doses of **3** (0.1 to 1.5 μM). At the end of the treatment, aliquots of each cell line were seeded into 60 mm plates and, after 10–12 days, colonies were stained with 2% methylene blue in 95% ethanol and counted (>50 cells equaled one colony).

Statistical analysis: The experiments have been repeated from three to five times and the results obtained are presented as mean standard deviations (±SD). Significant changes were assessed by using the Student's t-test for unpaired data, and P values <0.05 were considered significant.

Acknowledgements

This work was supported by the Italian Ministry of Education, University and Research (MIUR) Program for Research of National Interest (PRIN), the Sapienza Università di Roma, Italian Association for Cancer Research (AIRC) (grant no. 8633 and 11567) and the Italian Ministry of Health. S.I. is recipient of a fellowship from the Italian Foundation for Cancer Research (FIRC).

Keywords: antitumor agents · biological activity · cancer · DNA damage · G-quadruplexes

[1] a) S. Burge, G. N. Parkinson, P. Hazel, A. K. Todd, S. Neidle, *Nucleic Acids Res.* **2006**, *34*, 5402–5415; b) H. J. Lipps, D. Rhodes, *Trends Cell Biol.* **2009**, *19*, 414–422.

[2] a) S. Neidle, G. N. Parkinson, *Biochimie* **2008**, *90*, 1184–1196; b) D. Yang, K. Okamoto, *Future Med. Chem.* **2010**, *2*, 619–646; c) S. Neidle, G. N. Parkinson, *Nat. Rev. Drug Discovery* **2002**, *1*, 383–393.

[3] S. Neidle, *FEBS J.* **2010**, *277*, 1118–1125.

[4] M. Franceschin, *Eur. J. Org. Chem.* **2009**, 2225–2238.

[5] a) D. Drygin, A. Siddiqui-Jain, S. O'Brien, M. Schwaebe, A. Lin, J. Bliesath, C. B. Ho, C. Proffitt, K. Trent, J. P. Whitten, J. K. Lim, D. Von Hoff, K. Anderes, W. G. Rice, *Cancer Res.* **2009**, *69*, 7653–7661; b) P. J. Bates, D. A. Laber, D. M. Miller, S. D. Thomas, J. O. Trent, *Exp. Mol. Pathol.* **2009**, *86*, 151–164.

[6] a) N. Temime-Smaali, L. Guittat, A. Sidibe, K. Shin-ya, C. Trentesaux, J. F. Riou, *PLoS One* **2009**, *4*, e6919; b) L. R. Gauthier, C. Granotier, F. Hoffschir, O. Etienne, A. Ayouaz, C. Desmaze, P. Mailliet, D. S. Biard, F. D. Boussin, *Cell. Mol. Life Sci.* **2012**, *69*, 629–640; c) J. F. Riou, *Curr. Med. Chem. Anticancer Agents* **2004**, *4*, 439–443.

[7] a) E. Salvati, C. Leonetti, A. Rizzo, M. Scarsella, M. Mottolese, R. Galati, I. Sperduti, M. F. Stevens, M. D'Incalci, M. Blasco, G. Chiorino, S. Bauwens, B. Horard, E. Gilson, A. Stoppacciaro, G. Zupi, A. Biroccio, *J. Clin. Invest.* **2007**, *117*, 3236–3247; b) A. Rizzo, E. Salvati, M. Porru, C. D'Angelo, M. F. Stevens, M. D'Incalci, C. Leonetti, E. Gilson, G. Zupi, A. Biroccio, *Nucleic Acids Res.* **2009**, *37*, 5353–5364; c) E. Salvati, M. Scarsella, M. Porru, A. Rizzo, S. Iachettini, L. Tentori, G. Graziani, M. D'Incalci, M. F. Stevens, A. Orlandi, D. Passeri, E. Gilson, G. Zupi, C. Leonetti, A. Biroccio, *Oncogene* **2010**, *29*, 6280–6293.

[8] V. Casagrande, E. Salvati, A. Alvino, A. Bianco, A. Ciammaichella, C. D'Angelo, L. Ginnari-Satriani, A. M. Serrilli, S. Iachettini, C. Leonetti, S. Neidle, G. Ortaggi, M. Porru, A. Rizzo, M. Franceschin, A. Biroccio, *J. Med. Chem.* **2011**, *54*, 1140–1156.

[9] M. Franceschin, A. Alvino, V. Casagrande, C. Mauriello, E. Pascucci, M. Savino, G. Ortaggi, A. Bianco, *Bioorg. Med. Chem.* **2007**, *15*, 1848–1858.

[10] a) F. Rosu, E. De Pauw, V. Gabelica, *Biochimie* **2008**, *90*, 1074–1087; b) C. L. Mazzitelli, J. S. Brodbelt, J. T. Kern, M. Rodriguez, S. M. Kerwin, *J. Am. Soc. Mass Spectrom.* **2006**, *17*, 593–604; c) F. Rosu, V. Gabelica, C. Houssier, P. Colson, E. D. Pauw, *Rapid Commun. Mass Spectrom.* **2002**, *16*, 1729–1736; d) V. Casagrande, A. Alvino, A. Bianco, G. Ortaggi, M. Franceschin, *J. Mass Spectrom.* **2009**, *44*, 530–540.

[11] M. Franceschin, A. Alvino, G. Ortaggi, A. Bianco, *Tetrahedron Lett.* **2004**, *45*, 9015–9020.

[12] A. Alvino, M. Franceschin, C. Cefaro, S. Borioni, G. Ortaggi, A. Bianco, *Tetrahedron* **2007**, *63*, 7858–7865.

[13] a) U. Rohr, P. Schlichting, A. Bohm, M. Gross, K. Meerholz, C. Brauchle, K. Mullen, *Angew. Chem.* **1998**, *110*, 1463 – 1467; *Angew. Chem. Int. Ed.* **1998**, *37*, 1434 – 1437; b) U. Rohr, C. Kohl, K. Mullen, A. van de Craats, J. Warman, *J. Mater. Chem.* **2001**, *11*, 1789 – 1799; c) K. Sonogashira, Y. Tohda, N. Hagihara, *Tetrahedron Lett.* **1975**, *16*, 4467 – 4470.
[14] L. Rossetti, M. Franceschin, A. Bianco, G. Ortaggi, M. Savino, *Bioorg. Med. Chem. Lett.* **2002**, *12*, 2527 – 2533.
[15] B. van Steensel, T. de Lange, *Nature* **1997**, *385*, 740 – 743.
[16] H. Takai, A. Smogorzewska, T. de Lange, *Curr. Biol.* **2003**, *13*, 1549 – 1556.
[17] E. H. Blackburn, *Nature* **2000**, *408*, 53 – 56.
[18] US National Cancer Institute (NCI)/National Institutes of Health (NIH) Developmental Therapeutics Program: http://dtp.nci.nih.gov (Last accessed: September 26, 2012).
[19] a) B. Cathers, D. Sun, L. Hurley, *Anti-Cancer Drug Des.* **1999**, *14*, 367 – 372; b) J. E. Reed, M. Gunaratnam, M. Beltran, A. P. Reszka, R. Vilar, S. Neidle, *Anal. Biochem.* **2008**, *380*, 99 – 105; c) A. De Cian, G. Cristofari, P. Reichenbach, E. De Lemos, D. Monchaud, M. P. Teulade-Fichou, K. Shin-Ya, L. Lacroix, J. Lingner, J. L. Mergny, *Proc. Natl. Acad. Sci. USA* **2007**, *104*, 17347 – 17352.
[20] a) G. Pennarun, C. Granotier, L. R. Gauthier, D. Gomez, F. Hoffschir, E. Mandine, J. F. Riou, J. L. Mergny, P. Mailliet, F. D. Boussin, *Oncogene* **2005**, *24*, 2917 – 2928; b) T. Miyazaki, Y. Pan, K. Joshi, D. Purohit, B. Hu, H. Demir, S. Mazumder, S. Okabe, T. Yamori, M. S. Viapiano, K. Shin-Ya, H. Seimiya, I. Nakano, *Clin Cancer Res.* **2012**, *18*, 1268 – 80.
[21] a) B. van Steensel, A. Smogorzewska, T. de Lange, *Cell* **1998**, *92*, 401 – 413; b) K. Ancelin, C. Brun, E. Gilson, *Bioessays* **1998**, *20*, 879 – 883; c) F. d'Adda di Fagagna, P. M. Reaper, L. Clay-Farrace, H. Fiegler, P. Carr, T. von Zglinicki, G. Saretzki, N. P. Carter, S. P. Jackson, *Nature* **2003**, *426*, 194 – 198; d) A. Biroccio, A. Rizzo, R. Elli, C. E. Koering, A. Belleville, B. Benassi, C. Leonetti, M. F. Stevens, M. D'Incalci, G. Zupi, E. Gilson, *Eur. J. Cancer* **2006**, *42*, 1881 – 1888; e) D. Loayza, T. De Lange, *Nature* **2003**, *423*, 1013 – 1018; f) D. Hockemeyer, A. J. Sfeir, J. W. Shay, W. E. Wright, T. de Lange, *EMBO J.* **2005**, *24*, 2667 – 2678.
[22] a) A. M. Burger, F. Dai, C. M. Schultes, A. P. Reszka, M. J. Moore, J. A. Double, S. Neidle, *Cancer Res.* **2005**, *65*, 1489 – 1496; b) T. Tauchi, K. Shin-ya, G. Sashida, M. Sumi, S. Okabe, J. H. Ohyashiki, K. Ohyashiki, *Oncogene* **2006**, *25*, 5719 – 5792.
[23] A. Biroccio, S. Amodei, B. Benassi, M. Scarsella, A. Cianciulli, M. Mottolese, D. Del Bufalo, C. Leonetti, G. Zupi, *Oncogene* **2002**, *21*, 3011 – 3019.

Received: July 16, 2012
Published online on October 24, 2012

